Supporting Information for:

# High Performance Inverse Opal Li-ion Battery with Paired Intercalation and Conversion Mode Electrodes

David McNulty[1], Hugh Geaney[1], Eileen Armstrong[1] and Colm O'Dwyer[1,2]*

[1] *Department of Chemistry, University College Cork, Cork, T12 YN60, Ireland*

[2] *Micro-Nano Systems Centre, Tyndall National Institute, Lee Maltings, Cork, T12 R5CP, Ireland*

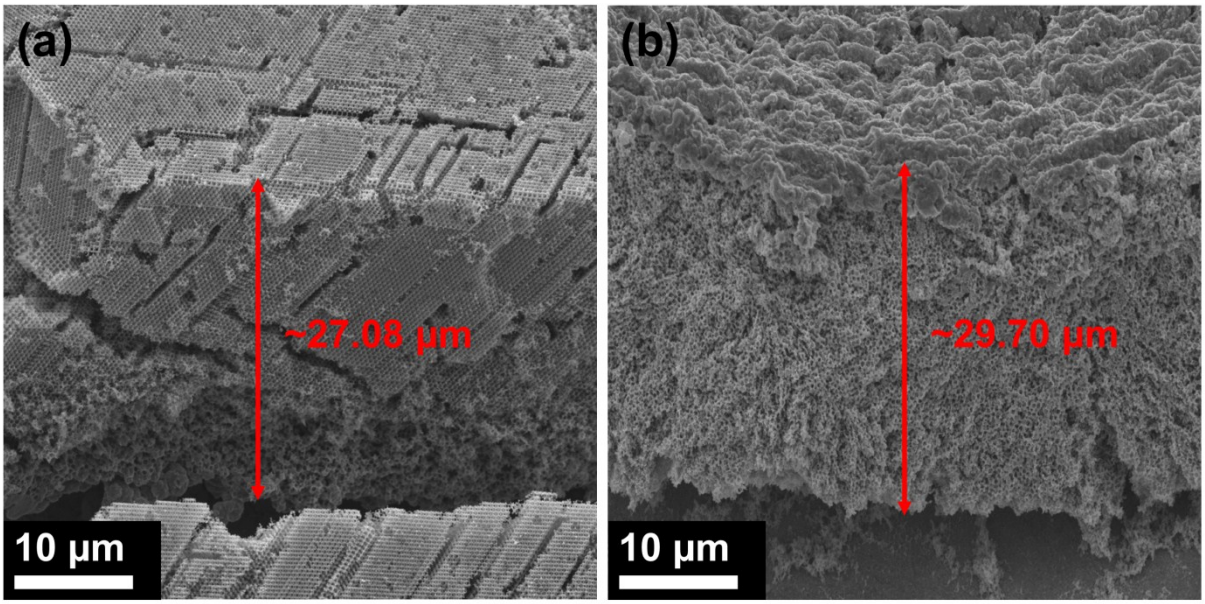


**Figure S1.** Tilt corrected SEM images of (a) a $V_2O_5$ inverse opal and (b) a $Co_3O_4$ inverse opal. Typical cross sectional thicknesses are indicated in each image by a red arrow.

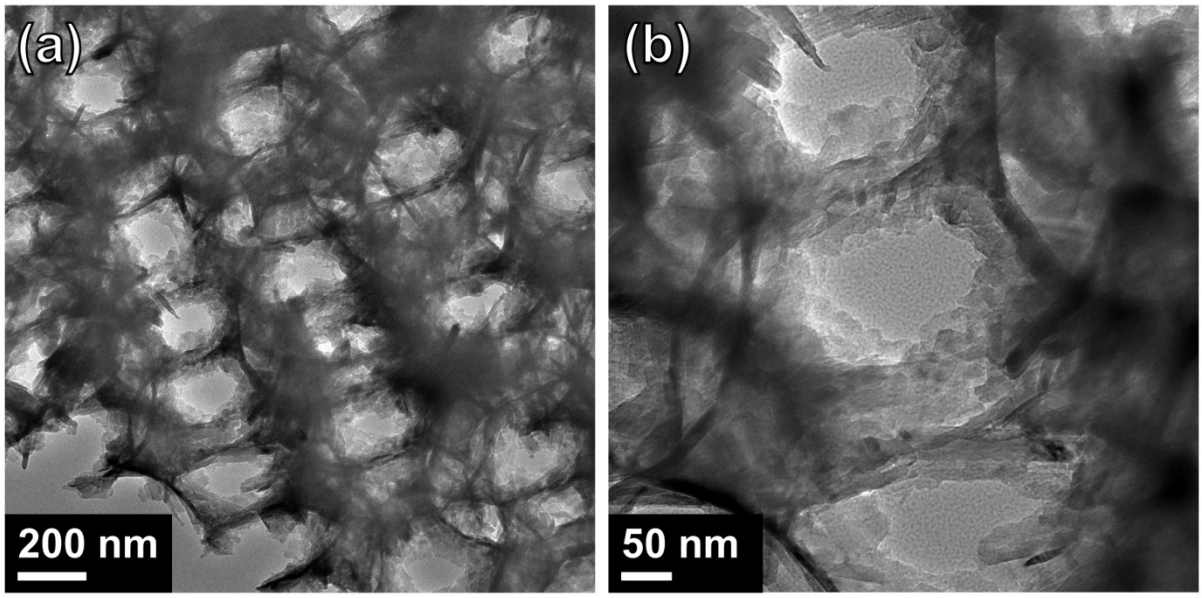


**Figure S2.** (a) and (b) TEM images of $V_2O_5$ inverse opals. The walls of the IO structure are comprised of an agglomeration of nanoscale crystallites of vanadium oxide.

A structural characterization of the $Co_3O_4$ IO material is presented in Figure S3. SEM images of the $Co_3O_4$ IO are shown in Figure S3a and b. Figure S3a shows large regions of the IO network. It is worth noting that it is not one continuous network on the stainless steel substrate, rather there are cracks in the IO network which have led to the formation of islands of IO material. These islands may be beneficial from an electrochemical point of view, ensuring that more of the IO network is in direct contact with the electrolyte. The crack characteristic of IO formation is typical, but electrical connectivity through the material is maintained by a strong adhesion to the metallic current collector. The diameter of the PS spheres was ~ 500 nm, after calcination of the infilled sphere template samples, this resulted in an IO network with pore sizes < 500 nm, as shown in Figure 3b. TEM and SAED images of the $Co_3O_4$ IO are shown in Figure S3c. The walls of the IO structure shown in detail in Figure 3c, mimics the opal template, and consists of an agglomeration of nano-sized crystalline grains of fcc $Co_3O_4$ identified via electron diffraction. The polycrystalline structure of the $Co_3O_4$ IO is confirmed by the presence of concentric circles in the SAED

pattern, which is indexed in the inset of Figure 3c. The $Co_3O_4$ IO XRD pattern is shown in Figure 3d. The three reflections with the highest intensity (labelled #) are stainless steel peaks and are present as a result of the $Co_3O_4$ IO samples being prepared on a stainless steel substrate. The remaining reflections have been successfully indexed to pure fcc $Co_3O_4$ (JCPDS No. 42-1467).

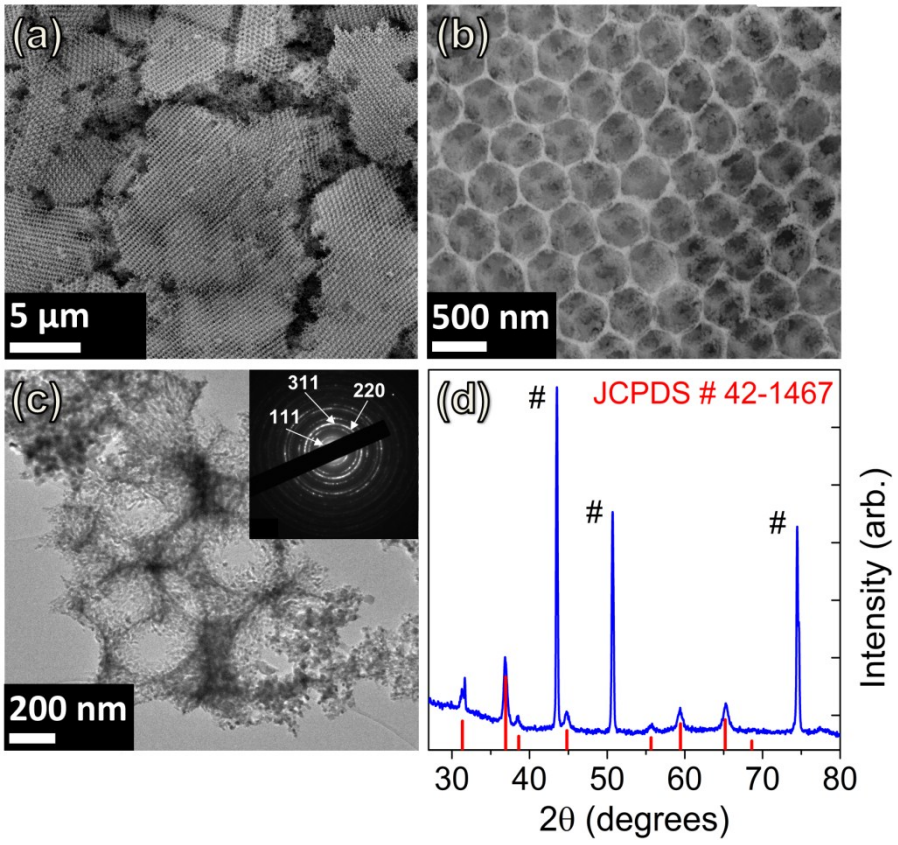


**Figure S3**. SEM images (a) and (b), TEM image (c) (SAED Inset) and XRD pattern (d) of $Co_3O_4$ IO, indexed to pure fcc $Co_3O_4$ (JCPDS No. 42-1467).

In this work, the electrochemical performance of a $Co_3O_4$ IO as an anode material in a half cell against a pure lithium counter electrode is evaluated. Cyclic voltammetry scans using a scan rate of 0.1 mV/s are shown in Figure S4. In the first cycle a well-defined reduction peak is observed at ~ 0.90 V, followed by a lower intensity peak at ~ 0.78 V, as shown in Figure S4. These peaks have previously been attributed to the initial irreversible reduction reaction of $Co_3O_4$ to Co [1, 2], according to:

$$Co_3O_4 + 8Li^+ + 8e^- \rightarrow 3Co + 4Li_2O \qquad \text{(Eqn S1)}$$

There is a decomposition of the $Co_3O_4$ electrode into a composite consisting of nanosized grains of Co embedded in a $Li_2O$ matrix. There are two obvious anodic peaks in the first scan at ~ 1.60 and 2.05 V, which may be attributed to the oxidation of Co to CoO [3] in the presence of $Li_2O$, as

$$Co + Li_2O \rightarrow CoO + 2Li^+ + 2e^- \qquad \text{(Eqn S2)}$$

For subsequent cycles, following the initial irreversible reduction of $Co_3O_4$ to Co, the insertion and removal of Li can be described as follows [4]

$$CoO + 2Li^+ + 2e^- \leftrightarrow Co + Li_2O \qquad \text{(Eqn S3)}$$

In this manner, $Co_3O_4$ charges and discharges by the reversible formation and decomposition of $Li_2O$. [4, 5] It has previously been suggested that Co has significant catalytic activity that tends to facilitate the reversible formation of $Li_2O$.

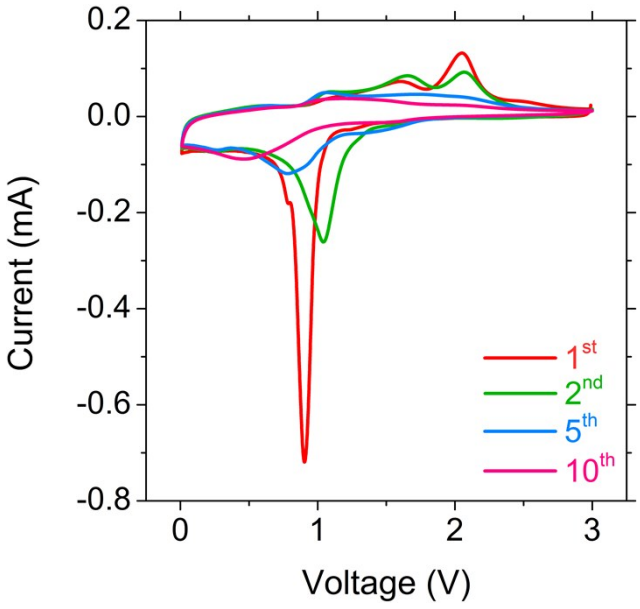


**Figure S4.** Cyclic voltammetry of a $Co_3O_4$ IO anode cycled in a half cell against pure Li metal, in a potential window of 3.0 – 0.01 V, using a scan rate of 0.1 mV $s^{-1}$.

This well-defined plateau is not present in subsequent cycles, indicating that the reaction as given in Eqn. S1, is indeed an irreversible reaction which occurs during the initial lithiation of the $Co_3O_4$ IO structure. The sloping decrease in the initial charge curve from ~1.05 V down to 0.01 V is often attributed to the formation of a "polymer–gel like film" within the interconnected porous nanostructure [4, 6-9], however this could be an incorrect assumption. This effect was first reported by Laruelle et al.[10], using cobalt oxide on a plastic laminate, which may be the cause of the polymer-gel film below 1 V. Hence, cobalt oxide IOs on stainless steel, aluminium or other metallic current collectors, prevent the formation of a polymer-gel film.

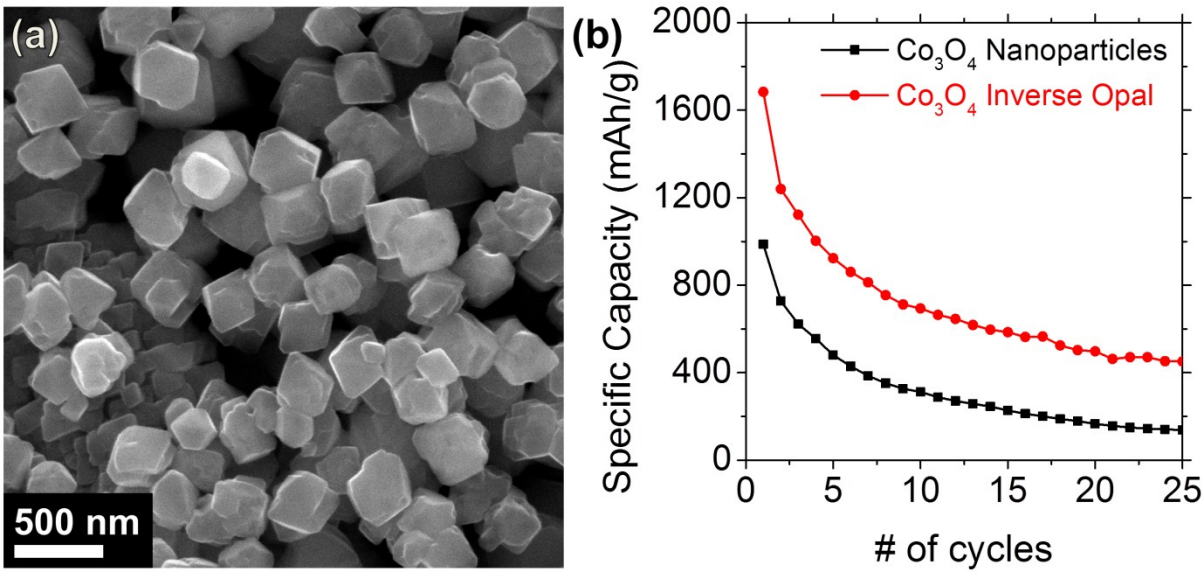


**Figure S5.** (a) SEM image of $Co_3O_4$ nanoparticles which are formed when a 0.1 M solution of $CoCl_2$ in IPA is dropcast onto a stainless steel current collector without a PS sphere template coating and then heated at 450 °C for 12 hours. (b) Specific capacity comparison for $Co_3O_4$ nanoparticles and a $Co_3O_4$ inverse opal sample over 25 cycles.

**References**


1. G. Huang, S. Xu, S. Lu, L. Li and H. Sun, *ACS Appl. Mater. Interfaces*, 2014, **6**, 7236-7243.
2. W.-Y. Li, L.-N. Xu and J. Chen, *Adv. Funct. Mater.*, 2005, **15**, 851-857.

3. Y. Zheng, L. Qiao, J. Tang, Z. Yang, H. Yue and D. He, *RSC Adv.*, 2015, **5**, 36117-36121.
4. D. Larcher, G. Sudant, J. Leriche, Y. Chabre and J. Tarascon, *J. Electrochem. Soc.*, 2002, **149**, A234-A241.
5. Y.-M. Kang, M.-S. Song, J.-H. Kim, H.-S. Kim, M.-S. Park, J.-Y. Lee, H. K. Liu and S. X. Dou, *Electrochim. Acta*, 2005, **50**, 3667-3673.
6. X. Wang, X. L. Wu, Y. G. Guo, Y. Zhong, X. Cao, Y. Ma and J. Yao, *Adv. Funct. Mater.*, 2010, **20**, 1680-1686.
7. S. A. Needham, G. Wang, K. Konstantinov, Y. Tournayre, Z. Lao and H. K. Liu, *Electrochem. Solid-State Lett.*, 2006, **9**, A315-A319.
8. J. Park, G.-P. Kim, H. N. Umh, I. Nam, S. Park, Y. Kim and J. Yi, *J. Nanopart. Res.*, 2013, **15**, 1-9.
9. K. M. Shaju, F. Jiao, A. Débart and P. G. Bruce, *Phys. Chem. Chem. Phys.*, 2007, **9**, 1837-1842.
10. S. Laruelle, S. Grugeon, P. Poizot, M. Dolle, L. Dupont and J. Tarascon, *J. Electrochem. Soc.*, 2002, **149**, A627-A634.